FT-EPR Study of the Wavelength Dependence of the Photochemistry of Phenols

Alejandro Bussandri and Hans van Willigen*

Department of Chemistry, University of Massachusetts at Boston, Boston, Massachusetts 02125

Received: September 13, 2001; In Final Form: December 4, 2001

The excitation wavelength dependence of the photochemistry of phenol, *p*-cresol, and tyrosine in neutral and acidic aqueous solution was examined using Fourier Transform Electron Paramagnetic Resonance (FT-EPR). Photoexcitation gives rise to formation of phenoxyl, *p*-cresyl, or tyrosyl radicals ($PhO^{\bullet}$), hydrated electrons (e^-_{aq}), and hydrogen atoms ($H^{\bullet}$). From Chemically Induced Dynamic Electron Polarization (CIDEP) effects and the effect of addition of N_2O on the spectra it can be deduced that the mechanism of hydrogen atom formation depends on the wavelength of excitation. Excitation into the S_2 absorption band ($\lambda_{ex} = 193$ nm) gives rise to H-atom formation by O−H bond homolysis and by e^-_{aq} capture by protons. The electron capture reaction produces a net absorption signal contribution in the FT-EPR spectrum of $H^{\bullet}$ due to transfer of spin polarization from e^-_{aq}. This demonstrates that the reaction occurs with H^+ in the bulk of the solution. The spectrum of $H^{\bullet}$ produced by excitation into the S_1 band ($\lambda_{ex} = 266$ nm) can be completely quenched by addition of N_2O. In this case H-atom formation is due entirely to the reaction of e^-_{aq} with H^+. The excitation energy apparently is insufficient to cause O−H bond cleavage. The spectra show no evidence of an in-cage H-atom formation mechanism such as $^1PhOH^* \rightarrow [PhOH^+\cdots e^-_{aq}] \rightarrow [PhO^{\bullet}\cdots H^{\bullet}] \rightarrow PhO^{\bullet} + H^{\bullet}$. Excitation to S_1 also leads to triplet-state formation. FT-EPR spectra show that triplet-state phenol (*p*-cresol) reacts with ground-state phenol (*p*-cresol) to give a cyclohexadienyl-type radical and $PhO^{\bullet}$.

I. Introduction

Previous work carried out on phenol and substituted phenols shows that the photochemical properties of these compounds are a sensitive function of reaction conditions.[1] Photoexcitation can lead to photoionization and hydrogen atom formation. The quantum yields of these two reaction paths depend on solvent, on the pH of the solution, and on wavelength of excitation.[2] In neutral or acidic aqueous solution, excitation of phenol into the S_1 absorption band leads primarily to photoionization (quantum yield $Q_e = 0.03$). H-atom formation is a very minor path ($Q_H \leq 0.002$). These quantum yields increase to 0.060 and 0.079, respectively, with excitation into the S_2 band.[2] The increase is accompanied by a decrease in quantum yield of fluorescence.[3] This demonstrates that the photochemistry of phenolic compounds can take place from electronic states above S_1 in competition with relaxation to the fluorescent state.[2,4] Excitation to S_1 is believed to open a reaction pathway via the fluorescent state.[2] Both pathways have been shown to be monophotonic.[2]

The present study was initiated with the objective to get more detailed information on the mechanisms of the photoinduced electron ejection and O−H bond homolysis reactions through Fourier Transform EPR (FT-EPR) spectra of the paramagnetic reaction products. In particular, the focus was on the effect of wavelength of excitation on Chemically Induced Dynamic Electron Polarization (CIDEP).[5] CIDEP effects in time-resolved EPR spectra give information on the spin state and spin dynamics of precursors of the free radicals monitored. A change in reaction path due to a change in excitation wavelength, therefore, may cause a change in spin polarization pattern. A wavelength dependence of CIDEP can be an important source of mechanistic information.[6−8]

In earlier time-resolved EPR studies of photoionization of phenolates in aqueous solution (pH 11), it was found that the spectra of the phenoxyl radicals and hydrated electrons display a low-frequency absorption/high-frequency emission (A/E) CIDEP pattern.[9−11] This pattern is independent of λ_{ex}.[11] The A/E polarization is generated by the spin state evolution in the transient radical pair $[PhO^{\bullet}\cdots e^-_{aq}]$. Generally, an A/E pattern is characteristic of a radical pair "born" with a triplet spin state, i.e., via a photoexcited triplet state.[5] However, in this case time-resolved EPR data[9,11] combined with the result of a picosecond transient absorption study[12] show that electron ejection must occur from a singlet excited state. To account for the unusual polarization pattern in the EPR spectra, the exchange interaction *J* between the unpaired electrons must be positive, i.e., the triplet radical pair state lies below the singlet state.[5]

One of the questions addressed in the present study is whether the pH affects the unusual polarization pattern observed for phenols (phenol, *p*-cresol, tyrosine) in alkaline aqueous solution.[9−11] The reaction path in neutral or acidic solution may differ from that in alkaline solution. Also, the spin state evolution of the radical pair formed by electron ejection may be affected by the presence of the proton of the hydroxyl group at the time of excitation. Finally, a change in excitation wavelength from 266 nm (used for excitation to S_1) to 193 nm (excitation to S_2) represents an energy difference of 1.8 eV that has to be dissipated by the system. The question is whether this affects radical pair characteristics.

A final point of interest is the mechanism of H-atom formation. In the studies of Grabner et al.,[1,2] quantum yields of e^-_{aq} and $H^{\bullet}$ formation were determined by measuring N_2 and H_2 gas evolution during continuous photolysis of solutions of the phenols. N_2 was generated by reacting e^-_{aq} with the scavenger N_2O, H_2 in a reaction of $H^{\bullet}$ with an alcohol. Under the

* Corresponding author. E-mail: hans.vanwilligen@umb.edu.

10.1021/jp013526u CCC: $22.00
Published on Web 02/05/2002

conditions of the measurements, electron scavenging by N_2O ($k = 5.6 \times 10^9$ M^{-1} s^{-1} [13]) is fast enough to suppress H-atom formation by the reaction of e^-_{aq} with protons in the bulk of the solution ($k = 2 \times 10^{10}$ M^{-1} s^{-1} [14]). However, H• can be formed as well in an "in-cage" two-step reaction sequence

$$^1\text{PhOH}^* \rightarrow [\text{PhOH}^+ \cdots e^-_{aq}] \rightarrow [\text{PhO}^\bullet \cdots \text{H}^\bullet]$$

The rate of this process may be fast enough to be competitive with electron scavenging by N_2O. The steady-state measurements provide no information on whether H-atom formation occurs by direct O−H bond homolysis and/or by electron capture. They also do not reveal if the pronounced change in quantum yield upon a change in excitation wavelength reflects a change in the mechanism of H• formation. CIDEP effects can give answers to these questions.

II. Experimental Section

Phenol from Aldrich (98%) was purified by sublimation; *p*-cresol (Aldrich, 99%) and tyrosine (Ajinomoto Co.) were used without further purification. Unless noted otherwise, measurements were carried out on solutions with a concentration of 1×10^{-3} M. Aqueous solutions were prepared with water from a Millipore Milli-Q purification system. The pH of the solutions was adjusted with KOH or HCl. Solutions, deoxygenated with argon gas, were pumped through a flat quartz cell held in the microwave cavity. In electron scavenging experiments, solutions were purged with N_2O gas.

Samples were excited with 193 nm UV-light from a Lambda Physik Compex 102 ArF excimer laser (∼15 ns pulse width, ∼20 mJ/pulse, 10 Hz) or 266 nm UV-light from a Quanta-Ray GCR-14S Nd:YAG laser (∼8 ns pulse width, 20 mJ/pulse, 10 Hz).

FT-EPR measurements were performed with the in-house-built instrument described before.[15] The response of the sample to the $\pi/2$ microwave pulse (∼15 ns) was detected in quadrature with application of the CYCLOPS phase-cycling routine. Since spectra cover a frequency range exceeding the bandwidth of the spectrometer, they are assembled from data recorded with a range of field settings. FIDs were recorded for a series of delay times ($10 \text{ ns} < \tau_d < 100\ \mu\text{s}$) between laser excitation and microwave pulse. For each field setting, the FIDs generally were the time average of signals generated by a total of 400 laser shots. Amplitudes, phases, and line widths of resonance peaks were derived from the FIDs with a LPSVD analysis routine.[16] By periodically repeating measurements carried out for a given field setting/delay time combination, it was verified that measurement conditions remained unchanged over the course of an experiment. All measurements were performed at room temperature.

III. Results

III.1. Excitation to S_1 (λ_{exc} = 266 nm). FT-EPR spectra given by aqueous solutions of phenol (1×10^{-3} M) with pH ranging from 11 to 2 upon photoexcitation into the first absorption band are shown in Figure 1. The spectra were recorded with an 80 ns delay time between laser and $\pi/2$ microwave pulses and show the presence of three paramagnetic species: solvated electron (e^-_{aq}), phenoxyl radical (PhO•), and hydrogen atom (H•). The absorption peak ($g = 2.000$) observed from pH 11 to pH 3 corresponds to e^-_{aq}.[9] The multi-line spectrum ($g = 2.0040$) with low-frequency absorption/high-frequency emission (A/E) pattern with the inversion point at the e^-_{aq} resonance position corresponds to PhO•.[9] The doublet observed from pH 7 to 2, with a peak separation of 50.586 mT (1416.4 MHz) and A/E spin polarization pattern, is the characteristic EPR spectrum of the hydrogen atom.[17] Similar spectra were observed upon photoexcitation of *p*-cresol and tyrosine in aqueous solution, the only difference being the hyperfine pattern in the spectra of the phenoxyl radicals.[11]

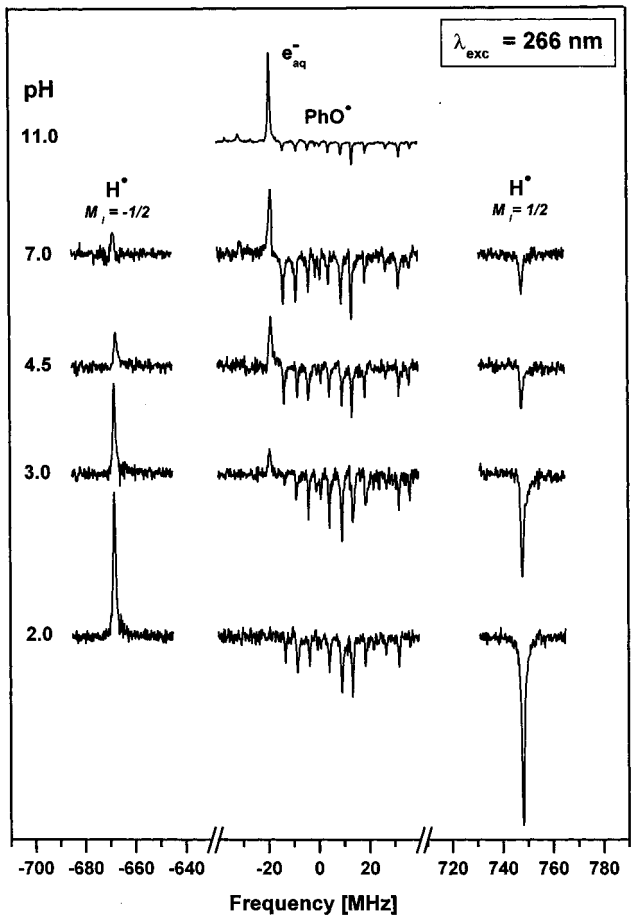

Figure 1. FT-EPR signals observed upon photoexcitation of 10^{-3} M phenol in aqueous solution at different pH. Excitation wavelength 266 nm (20 mJ), 80 ns delay-time between microwave and laser pulses. Absorption peaks point up, emission peaks down. Spectra are the time average produced by 400 laser shots. The frequency axis is given with respect to the center of the PhO• spectrum.

Figure 1 shows that the spectrum generated by PhO•, and e^-_{aq} at pH 7 is qualitatively similar to that at pH 11. However, integration of the spectrum obtained at pH 11 shows that overall net spin polarization is close to zero,[11] establishing that signal intensity is controlled by ST_0 radical pair mechanism (RPM) CIDEP.[5] On the other hand, at pH 7 the central portion (−40 to +40 MHz) of the spectrum shows a distinct net emission contribution (A/E* pattern). Even so, the PhO• resonance peaks still turn from absorption to emission at the position of the e^-_{aq} resonance establishing that the $[\text{PhO}^\bullet \cdots e^-_{aq}]$ geminate radical pair remains the dominant source of CIDEP for these radicals.

The intensity of the e^-_{aq} resonance decreases by about 77% upon going from pH 11 to pH 7. This result is in close agreement with the 82% decrease in quantum yield of e^-_{aq} formation (λ_{exc} = 254 nm) measured by Grabner et al.[2] It is evident from the spectra displayed in Figure 1 that the intensity of the PhO• spectrum is less dependent on pH so that there is a pronounced change in the relative intensities of the signals due to e^-_{aq} and PhO•.

Figure 1 illustrates that further decreases in pH by addition of HCl cause additional decreases in e^-_{aq} signal intensity. At pH 2 this signal is no longer observed. The attenuation of the e^-_{aq} resonance is attributed to scavenging of the hydrated electron by protons, $e^-_{aq} + H^+ \rightarrow H^\bullet$. This reaction has a rate constant of about 2.3×10^{10} M^{-1} s^{-1}.[14] Therefore, the lifetime of e^-_{aq} at pH 2 is ~5 ns which is too short to allow its detection with FT-EPR because of the dead time of the spectrometer (~ 120 ns). The line width of the e^-_{aq} peak increases with decreasing pH, reflecting the decrease in lifetime of this species.

The $PhO^\bullet$ spectrum maintains a more or less constant polarization pattern in the pH 7−2 range with the emission portion of the spectrum on the high-frequency side of the e^-_{aq} resonance peak. This establishes that the mechanism of $PhO^\bullet$ formation at pH 2 still involves the $[PhO^\bullet \cdots e^-_{aq}]$ radical pair. Optical studies have shown that Q_e remains constant over the pH 7 to 1 range.[2] As shown in Figure 1, the intensity of the $PhO^\bullet$ spectrum remains essentially unchanged over this pH range as well. From this it is concluded that photoionization is the major channel of phenoxyl radical formation over the entire pH range.

The decrease of the intensity of the e^-_{aq} signal as the pH is reduced from 7 to 2 is accompanied by a hydrogen atom spectrum that rapidly increases in intensity (cf. Figure 1). Over the entire pH range that the $H^\bullet$ spectrum can be observed it exhibits a low-frequency absorption/high-frequency emission pattern with a net overall emission signal contribution (A/E* pattern) independent of delay time setting. At pH 2 the intensity of the emissive high-frequency line is about 20% higher than the intensity of the low-frequency absorption line.

As the delay time between laser excitation and microwave pulses is increased, a series of additional peaks gradually grows in. The paramagnetic species responsible for this new spectrum, that covers a frequency range of about 320 MHz and also exhibits an A/E polarization pattern, is formed over a time period of 1−2 μs. Over this time period, the transition from absorption to emission in the spectrum $PhO^\bullet$ shifts from the e^-_{aq} peak position to the center of this new spectrum.

The spectrum obtained at pH 2 with $\tau_d = 1.5$ μs, which shows resonance peaks due to the phenoxyl radical and the new radical, is displayed in Figure 2a. The spectrum due to the new radical can be simulated with the following hyperfine coupling constants (hfcc's): 122.0 MHz (2H), 35.64 MHz (1H), 25.39 MHz (1H), 7.03 MHz (1H), and 5.69 MHz (1H). The high-frequency wing of this spectrum and its simulation are displayed in the inset of Figure 2a. The polarization pattern of this spectrum, its rate of growth (see below), and the hfcc's point to a mechanism in which a pair of free radicals with similar *g* values is formed in a bi-molecular reaction. The mechanism that fits the experimental data is a H-abstraction reaction giving the phenoxyl radical and a cyclohexadienyl-type radical ($HPhOH^\bullet$).

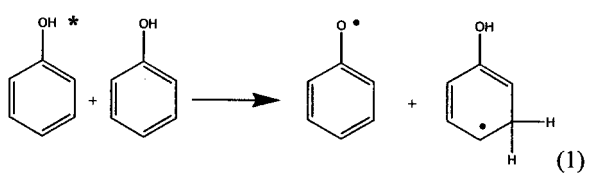

(1)

In agreement with this interpretation, the spectrum shown in Figure 2a can be accounted for in terms of a major (1:2:1) triplet splitting (hfcc 122 MHz) that is attributed to the CH_2 protons of $HPhOH^\bullet$ with additional smaller doublet splittings due to four (nonequivalent) protons. The value of the triplet splitting is in close agreement with the value of 134 MHz reported for the cyclohexadienyl radical.[18] Confirming this interpretation, it is found that photoexcitation of phenol in D_2O at pH 2 produces a radical that gives an EPR spectrum covering a strongly reduced spectral width (cf. Figure 2b). This spectrum can be simulated with the four hfcc's due to single protons given above, but replacing one H in CH_2 by D with $a_D = 18.7$ MHz ($a_H/a_D = 6.5$). The inset in Figure 2b shows the high-frequency wing of the spectrum together with the simulation of this region of the spectrum.

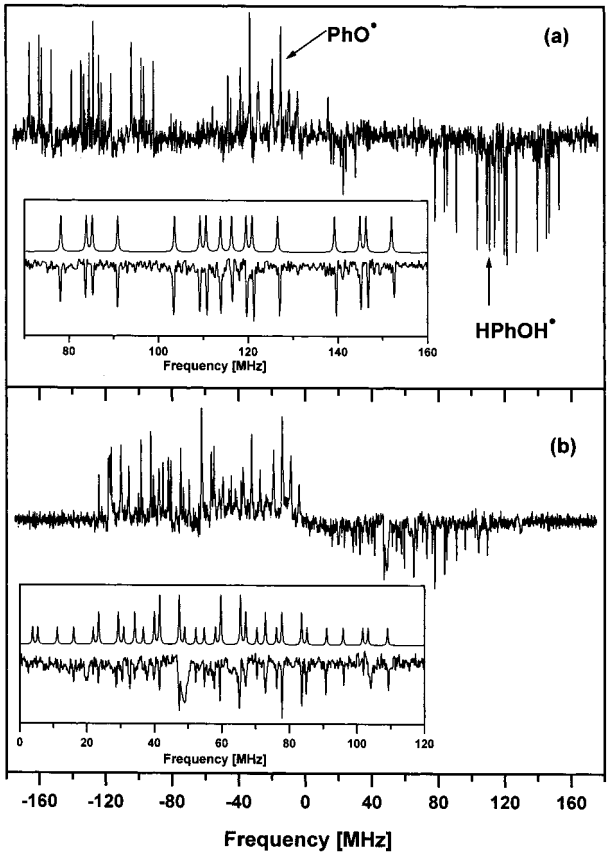

Figure 2. FT-EPR spectrum observed with a delay time setting of 1.5 μs upon photoexcitation ($\lambda_{exc} = 266$ nm, 20 mJ) of phenol (10^{-3} M) in (a) H_2O and (b) D_2O at pH 2. The insets show the high-frequency wings of the spectra and their simulation on the basis of the hfcc's given in the text. The arrows mark resonance peaks used to monitor signal growth and decay (cf. Figure 3).

The deuteration experiment establishes unequivocally that the radical formation step involves hydrogen (deuterium) atom transfer from the hydroxyl group of one phenol molecule to the phenyl ring of another. The EPR data establish that H-atom addition occurs preferentially at either the meta or ortho position. In accord with the proposed reaction mechanism, the switch from H_2O to D_2O does not affect the spectrum of the phenoxyl radical.

The cyclohexadienyl-type radical was observed upon S_1 (266 nm) photoexcitation of phenol and *p*-cresol solutions in the pH 7−2 range. As expected, given the mechanism of radical formation, the spectrum of this radical is not observed in basic solution.[11] A similar photoinduced hydrogen abstraction reaction has been found previously for sesamol (3,4-methylenedioxyphenol) in aqueous solution at pH 7−4.[19]

The time evolution of intensities of resonance peaks of the four paramagnetic species generated by excitation in the S_1 absorption band of phenol in neutral and acidic solutions is shown in Figure 3. The signals from e^-_{aq} and $PhO^\bullet$ develop

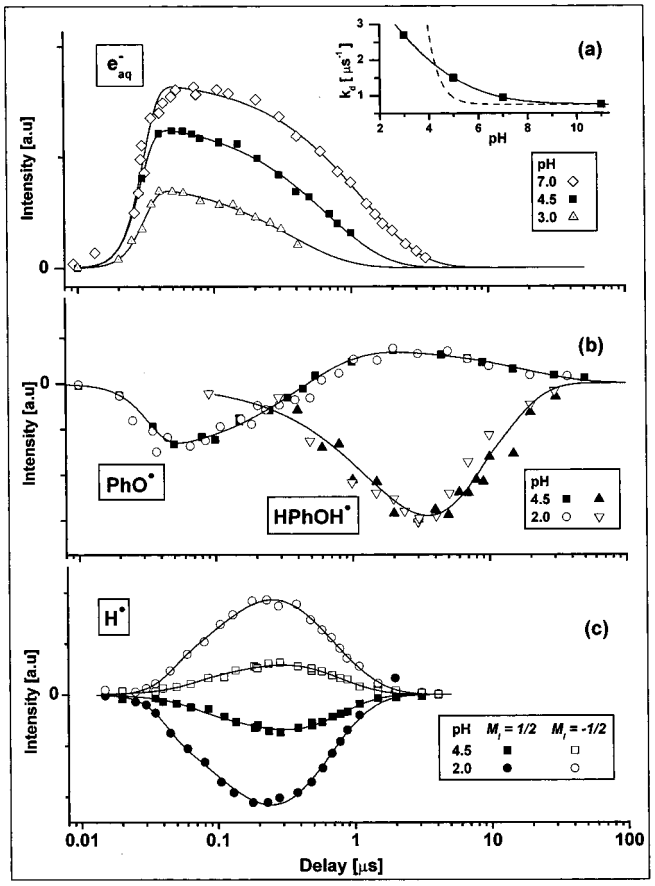

Figure 3. Time evolution of the intensities of resonance peaks of the four paramagnetic species formed by photoexcitation ($\lambda_{exc} = 266$ nm, 20 mJ) of phenol in neutral and acidic aqueous solutions. The resonance peaks in the spectra of PhO• and HPhOH• used to monitor the time dependence are marked by arrows in Figure 2a. The inset of Figure 3a shows the measured rates of decay of the e^-_{aq} signal as a function of pH. The dashed line represents the pH dependence predicted for the reaction $e^-_{aq} + H^+ \rightarrow H^\bullet$ (rate constant 2×10^{10} M^{-1} s^{-1}).

with a rate controlled by the instrument response ($\sim 4 \times 10^7$ s^{-1}). Scavenging of e^-_{aq} by protons is reflected in the increase of the rate of decay (k_d) as the pH of the solution is reduced (cf. Figure 3a). The inset in Figure 3a shows the pH dependence of k_d. It is evident that there is no linear dependence of k_d on [H^+] (dashed line inset Figure 3a). The lack of a linear relationship shows that other pH-dependent signal decay channels play a significant role. They can include spin−lattice relaxation and back-electron transfer.

Figure 3b shows the time evolution of the intensities of selected peaks (marked by arrows in Figure 2a) in the PhO• and HPhOH• spectra for pH values of 4.5 and 2. In this case, time profiles and signal intensities are independent of pH, contrary to what is found for e^-_{aq} and H• (see below). As mentioned above, the PhO• spectrum develops with instrument-controlled rise time. The selected peak in the spectrum of this radical turns from emission into absorption over a period of 1−2 μs because of a signal contribution due to the hydrogen abstraction reaction (reaction 1) and because of spin−lattice relaxation ($T_1 \approx 0.3$ μs).

Accompanying the change in the polarization pattern in the spectrum of PhO• is the development of the HPhOH• spectrum. This spectrum grows in over a period of ~ 2 μs ($k_f = 3.5 \times 10^5$ s^{-1}, cf. Figure 3b). It is evident from the time profiles given in Figure 3 that HPhOH• signal development is much slower than that of the other species. The lifetime of the singlet excited state

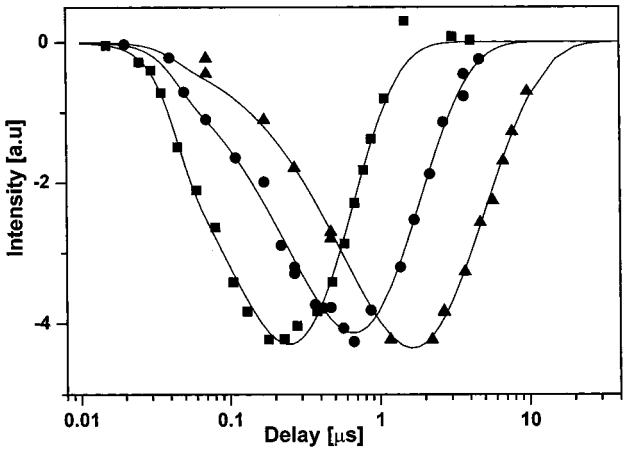

Figure 4. Time profiles of the signal intensity of the low-field hydrogen line observed upon excitation ($\lambda_{exc} = 266$ nm) of acidic (pH 2) aqueous solutions of phenol with concentrations of (■) 1×10^{-3} M, (●) 0.3×10^{-3} M, and (▲) 0.1×10^{-3} M.

of PhOH is of the order of = 0.3 ns,[12] so that it must be concluded that the hydrogen abstraction reaction which gives rise to HPhOH• involves the triplet excited state of the phenol.

The hydrogen atom spectrum maintains an A/E* spin polarization pattern over the entire time range that signals can be observed (cf. Figure 3c). The signal growth and decay can be described reasonably well with single exponentials. The rate of signal growth (k_g) is found to be dependent on pH, laser power, and [PhOH]. In contrast, signal decay (k_d) depends on [PhOH] only. With 20 mW laser power and [PhOH] = 1×10^{-3} M, k_g increases from $4.5(\pm 0.8) \times 10^6$ s^{-1} to $7.1(\pm 0.2) \times 10^6$ s^{-1} upon going from pH 4 to pH 2. Since these rates are near the instrument-controlled limit ($\sim 4 \times 10^7$ s^{-1}), the increase observed on decreasing the pH simply may reflect the increase in H-atom concentration rather than a change in chemical rate. In agreement with this interpretation, it is found that a decrease in laser power results in a decrease in signal growth rate.

Figure 4 displays the effect of varying the phenol concentration, at constant laser power (20 mW) and pH (2), on the time profile of the high-frequency H• resonance peak. It is found that the rate of signal growth is a linear function of [PhOH] with a slope of 6.2×10^9 M^{-1} s^{-1}. The rate of signal decay also depends linearly on [PhOH] with a slope of 2.3×10^9 M^{-1} s^{-1}. Signal decay is attributed to the reaction of the hydrogen atom with phenol for which a rate constant in the range of 1.8×10^9 to 2.1×10^9 M^{-1} s^{-1} has been reported.[21] Because of this H-atom quenching reaction, the spectrum can be observed only when the phenol concentration is $\leq 1 \times 10^{-3}$ M. At higher concentration the signal decays into the baseline within the deadtime of the spectrometer. The reaction of the H-atoms with phenol also must produce cyclohexadienyl-type radicals. However, no signal contribution from this reaction path could be identified in the spectra.

III.2. Excitation to S_2 ($\lambda_{exc} = 193$ nm). Figure 5 shows the FT-EPR spectra given by aqueous solutions of phenol for pH values ranging from 11 to 2.3 upon photoexcitation to S_2 for a delay time of 80 ns. The results obtained differ in a number of important aspects from those obtained upon excitation to S_1.

In this case, only the spectra of the three radicals e^-_{aq}, PhO•, and H• can be observed. The cyclohexadienyl-type radical HPhOH• was not observed at any delay time. The A/E spin polarization pattern in the e^-_{aq} and PhO• spectra is similar to

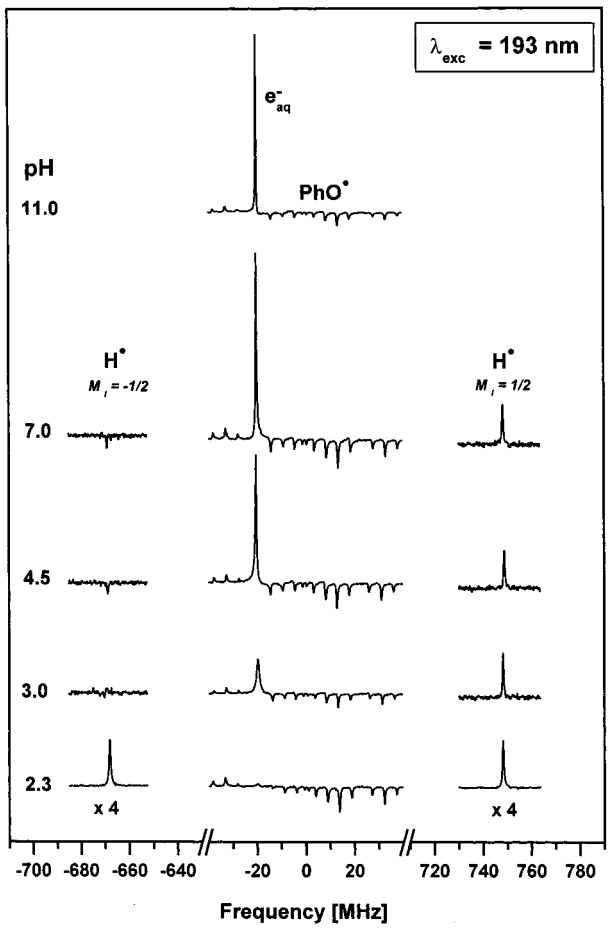

Figure 5. FT-EPR spectra observed upon photoexcitation of 10^{-3} M phenol in aqueous solution at different pH. Excitation wavelength 193 nm (~20 mJ), 80 ns delay time between microwave and laser pulses. Absorption peaks point up, emission peaks down. The signals are the time average produced by 400 laser shots. The frequency axis is given with respect to the center of PhO• spectrum. The H-atom signal intensities are expanded by a factor of 4.

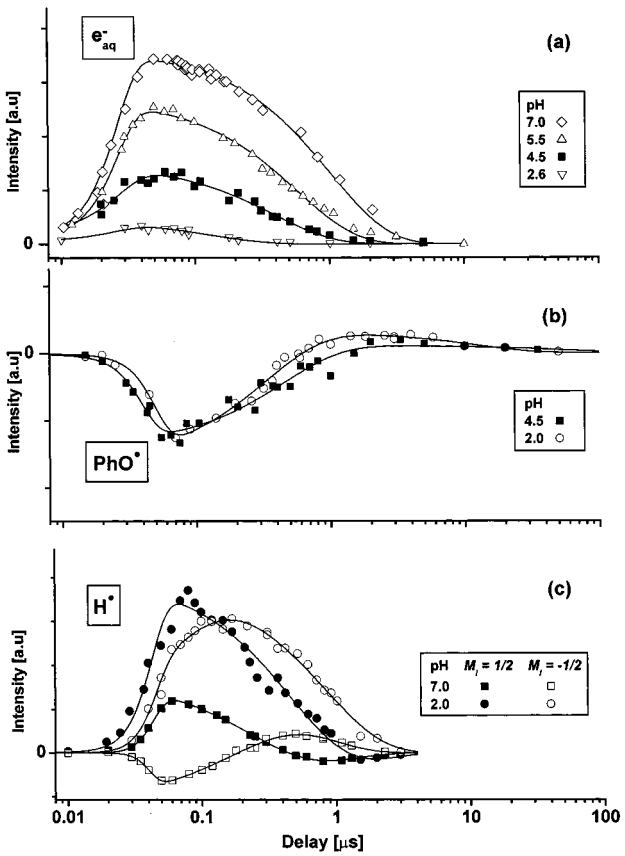

Figure 6. Time evolution of the intensities of resonance peaks from the three paramagnetic species generated by photoexcitation (λ_{exc} = 193 nm, ~20 mJ) of phenol.

that found upon excitation with 266 nm laser pulses. In contrast,a comparison of the spectra presented in Figures 1 and 5 shows that the change in excitation wavelength changes the spin polarization pattern in the H-atom spectrum. With 266 nm excitation it is found to be A/E* over the pH 7−2 range. Upon 193 nm excitation it is E/A* from pH 7 to 3 with the net absorption component growing in relative importance as the pH is reduced. At pH 2.3 the H• spectrum is completely in absorption.

The polarization pattern in the spectra of e_{aq}^- and PhO• show that the geminate radical pair [PhO•···e_{aq}^-] remains the dominant source of CIDEP over the entire pH range. The integral of the central portion of the spectrum (containing the resonance peaks from e_{aq}^- and PhO•) at pH 7 shows only a small net absorption component. In the case of 266 nm excitation, a significant net emission contribution is evident (cf. Figure 1).

The spectra of e_{aq}^- and PhO• obtained upon excitation to S_2 exhibit a much better signal-to-noise than those produced by S_1 excitation (cf. Figures 1 and 5). This is consistent with the reported increase in quantum yield of photoionization.[2] The e_{aq}^- signal intensity decreases with decreasing pH. As noted in the previous section, this is due to electron scavenging by H^+. At pH 2.3 the e_{aq}^- resonance is no longer observed because of the instrument dead time. Even so, the PhO• spectrum still shows the transition from absorption to emission at the e_{aq}^- resonance frequency, establishing that CIDEP is generated by the spin state evolution of the precursor [PhO•···e_{aq}^-] radical pair. Time profiles of PhO• and e_{aq}^- resonance peaks are depicted in Figure 6a,b. They are similar to those measured with 266 nm excitation (cf. Figure 3).

The spectra of H• produced by 193 nm excitation exhibit a time profile that is fundamentally different from that found upon excitation into the S_1 absorption band. As shown in Figure 6c, both hyperfine components now grow in with instrument-controlled rise time. At pH 7, the low frequency peak initially is in emission, the high-frequency peak in absorption. This pattern reverses to A/E for τ_d > 200 ns. At pH 2 both peaks start off in absorption, but with increasing delay time the pattern also evolves into A/E. The spectra shown in Figure 7 clearly illustrate the changes in polarization pattern associated with the change in excitation wavelength and increase in delay time.

FT-EPR measurements on *p*-cresol and tyrosine solutions excited with 193 nm light gave results identical to those presented for phenol.

III.3. Effects of e_{aq}^- Scavenging by N_2O. As pointed out in the Introduction, a question that may be answered with the FT-EPR measurements is whether H-atom formation occurs by direct photoinduced O−H bond homolysis or via a two-step process: photoionization of the phenol followed by electron capture by H^+ giving H•. In the latter case, H• can be generated in an in-cage reaction,

$$^1\text{PhOH}^* \rightarrow [\text{PhOH}^+\cdots e_{aq}^-] \rightarrow [\text{PhO}^\bullet\cdots \text{H}^\bullet] \rightarrow \text{PhO}^\bullet + \text{H}^\bullet$$

Alternatively, photoionization could be followed by fast dis-

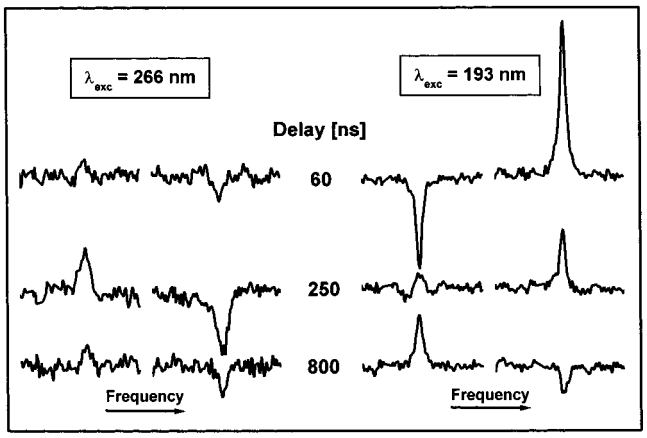

Figure 7. FT-EPR spectra of hydrogen atoms formed by photoexcitation of phenol in aqueous solution (pH 7) into its S_1 ($\lambda_{exc} = 266$ nm) and S_2 ($\lambda_{exc} = 193$ nm) absorption band for different delay times between the laser and microwave pulses. Absorption peaks point up, emission peaks down.

sociation of the proton, and eventual capture of the hydrated electron by protons in the bulk of the solution,

$$^1\text{PhOH}^* \rightarrow [\text{PhOH}^+\cdots e^-_{aq}] \rightarrow [\text{PhO}^\bullet\cdots e^-_{aq}] + H^+ \rightarrow \text{PhO}^\bullet + H^\bullet$$

To resolve the question of whether photoionization precedes H-atom generation, the effect of scavenging of the hydrated electron by N_2O was investigated.

The effect of bubbling N_2O gas through aqueous solutions of phenol with pH values in the 7−3 range is illustrated in Figure 8. In the case of excitation in the S_1 band (Figure 8a), the introduction of N_2O leads to a pronounced reduction in H$^\bullet$ signal intensity at pH 2. The relative intensity of the two hyperfine components changes slightly so that the polarization pattern appears to change from A/E* to A*/E. Above pH 2, the H-atom signal is completely quenched by addition of N_2O.

With excitation in the S_2 band, the H-atom spectrum remains visible over the entire pH range. Figure 8b shows that introduction of N_2O has little or no effect at pH 7, but removes or attenuates the net absorption signal contribution present at lower pH. The overall effect is that the polarization pattern goes toward E/A.

IV. Discussion

The change in excitation wavelength from 266 to 193 nm is found to cause significant changes in the FT-EPR spectra. Most notable are the following effects on the characteristics of the H$^\bullet$ spectrum: (*i*) a switch in the polarization pattern of the spectrum (cf. Figures 1 and 5); (*ii*) the change in the kinetics of H$^\bullet$ signal growth (cf. Figures 3 and 6); (*iii*) the difference in the effect of addition of the electron scavenger N_2O (cf. Figure 8). As will be discussed below, these changes reflect a fundamental change in the mechanism of H-atom formation. In the discussion, the data obtained with 193 nm excitation will be taken up first because they lend themselves most readily to a mechanistic interpretation.

IV.1. Excitation to S_2. The spectra of the PhO$^\bullet$ and e^-_{aq} radicals produced by 193 nm excitation of phenol (*p*-cresol, tyrosine) solutions (pH 11−2.3, Figure 5) exhibit a clear ST_0 RPM pattern due to the radical pair [PhO$^\bullet\cdots e^-_{aq}$]. On the other hand, at short delay time (80 ns), the H-atom spectrum shows E/A* polarization in the pH 7−3 range and is completely in absorption at pH 2.3. The pH dependence of the polarization pattern in the H$^\bullet$ spectrum shows that it is made up of two major contributions. An E/A contribution that dominates at pH 7 and a net absorption contribution that increases with increasing acidity of the solution.

The effect of electron scavenging by N_2O on the H$^\bullet$ spectra depicted in Figure 8b sheds light on the origin of these two CIDEP contributions. It is evident that N_2O addition attenuates the net absorption signal contribution. In the pH 7−3 range this leaves an E/A* pattern with a small net absorption component. At pH 2, a signal that is almost 1:1 absorption when the solution is purged with argon turns into E/A* when N_2O is introduced instead.

From the pH dependence of the net absorption contribution and its quenching by N_2O it can be concluded that it is due to H-atom formation by e^-_{aq} scavenging by protons in the bulk of the solution (rate constant 2.3×10^{10} M^{-1} s^{-1} [14]). The overall reaction sequence is

$$^1\text{PhOH}^* \rightarrow [\text{PhO}^\bullet\cdots e^-_{aq}] + H^+ \rightarrow \text{PhO}^\bullet + e^-_{aq} + H^+$$

$$e^-_{aq} + H^+ \rightarrow H^\bullet$$

In this process the spin polarization of the hydrated electrons, generated in the [PhO$^\bullet\cdots e^-_{aq}$] radical pair, is carried over to the hydrogen atoms, accounting for the net absorption signal. Electron scavenging by N_2O suppresses this reaction channel. At pH 2, the net absorption contribution is not completely removed (cf. Figure 8b). Apparently, the rates of electron scavenging by H^+ and N_2O are of comparable magnitude under those conditions.

The second channel of H-atom formation, giving rise to an E/A signal with small net A component, is not affected by N_2O addition showing that it is independent of the photoionization step. This signal contribution is attributed to direct photoinduced O−H bond homolysis via the S_2 excited state,

$$^1\text{PhOH}^*(S_2) \rightarrow [\text{PhO}^\bullet\cdots H^\bullet] \rightarrow \text{PhO}^\bullet + H^\bullet$$

The time profiles of H$^\bullet$ signal intensities (cf. Figure 6c) are in accord with this assignment. First, signal growth is instrument controlled. Second, the H$^\bullet$ spectrum at pH 7 develops with E/A polarization, but for $\tau_d > 0.5$ μs the pattern switches to A/E (cf. Figures 6c and 7). This time evolution of CIDEP is consistent with spin polarization generated first by the geminate pair ST_0 RPM operating in [PhO$^\bullet\cdots$H$^\bullet$] formed via the singlet excited state and subsequently by pairs formed in radical termination reactions (F-pair RPM CIDEP).[5] In the latter process, radical−radical encounters that produce pairs with singlet character react instantly leaving triplet pairs. The spin state evolution in these surviving pairs produces polarization opposite to that given by singlet geminate pairs.[5] From the polarization patterns it can be deduced that the exchange interaction J between the unpaired electrons in the radical pairs must be negative as is usually the case.

The fact that the spectra for pH 7−3 with N_2O purging (Figure 8b) display an E/A* pattern point to a spin polarization contribution from the ST_{-1} RPM. It has been shown that ST_{-1} mixing will play a significant role when one or more of the hfcc's are large.[5]

The spin state development in the [PhO$^\bullet\cdots$H$^\bullet$] geminate pairs also must produce an E/A signal contribution in the spectrum of the phenoxyl radicals. However, as shown in Figure 5, the spectrum of PhO$^\bullet$ maintains its polarization pattern unchanged

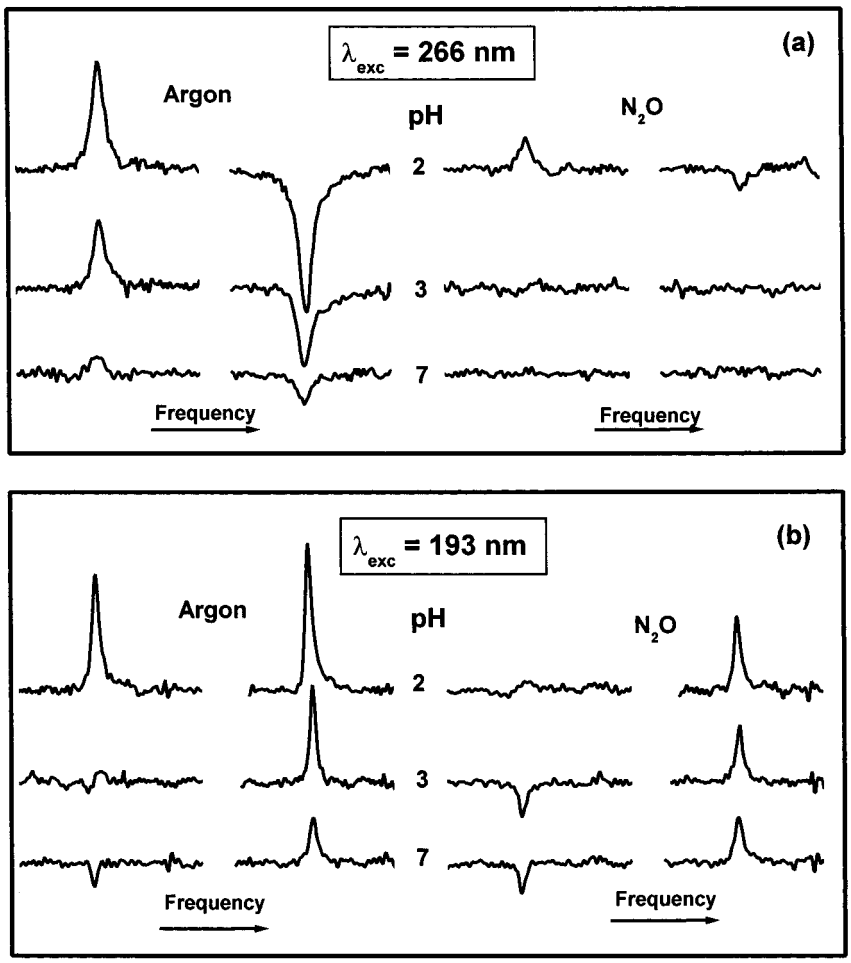

Figure 8. Spectra of H• formed by photoexcitation of aqueous solutions of phenol (pH 2, 3, and 7) with 266 nm (a) or 193 nm (b) laser light. Solutions bubbled with argon (left) or N_2O gas (right).

over the entire pH range. The integrals over the central portion of the spectra given by pH 11 and 7 solutions both are virtually zero, providing evidence that spin polarization generated by the [PhO•···e_{aq}^-] radical pair dominates irrespective of whether H• is formed or not. The absence of an effect of the bond homolysis reaction on the CIDEP pattern of the phenoxyl radical spectrum can be accounted for on the basis of RPM CIDEP theory.[21] According to this theory, the intensity of a resonance peak in the spectrum of H• is proportional to the square root of its frequency offset from the center of the PhO• spectrum. Similarly, that of a peak in the spectrum of PhO• depends on the square root of the frequency offset from the center of the spectrum due to H•. Given the large difference in hfcc's, signal contributions to the spectrum of PhO• stemming from [PhO•···H•] will be a very small fraction of the H• signal intensity.

IV.2. Excitation to S_1. Figure 1 shows that excitation of neutral or acidic solutions of phenol to S_1 (λ_{ex} = 266 nm) produces H-atoms that give rise to a spectrum with an A/E* polarization pattern. Similar results have been obtained with *p*-cresol and tyrosine. An A/E pattern with additional net emission contribution is found as well in the central part (−40 to +40 MHz) of the spectra comprising resonance peaks due to PhO• and e_{aq}^-.

As illustrated in Figure 8, introduction of N_2O leads to complete quenching of the H• resonance peaks (pH 7−3) or strong attenuation (pH 2). From this it must be concluded that the resonance peaks must be due to H• formed in a two-step process, photoionization followed by electron capture by H^+. Apparently, *the photon energy is insufficient to effect direct H-atom formation by O−H bond homolysis*.

Upon electron capture, the spin polarization of the hydrated electron will be transferred to the hydrogen atom which should give rise to a net absorption signal contribution in the spectrum of H• as is found for S_2 excitation (cf. Figures 5 and 8b). However, in this case an A/E* pattern is found over the pH 7−2 range. From the dependence of the kinetics of the development of this A/E* signal on phenol concentration (cf. Figure 4) it can be concluded that the origin of the spin polarization must be the F-pair RPM.[5] With increasing phenol concentration, the concentration of radicals generated by a laser shot increases. This, in turn, leads to an increase in the rate of radical termination reactions which is reflected in a faster development of spin polarization. The fact that for a delay time of 800 ns the polarization patterns in the 193 nm/pH 7 and 266 nm/pH 7 spectra are identical (cf. Figure 7) is in agreement with this interpretation. F-pair RPM as a source of spin polarization is also consistent with the finding that the H-atom spectrum shows a significant net emission component. This component stems from ST_{-1} mixing in [PhO•···H•] radical pairs "born" in the triplet state.

The lack of a noticeable net absorption contribution in the H• spectra due to transfer of spin polarization from the hydrated electrons may be due to the relatively weak e_{aq}^- signal. If the H-atoms are formed exclusively in the reaction of e_{aq}^- with H^+, the H-atom resonance peak intensity at best can be half that of the e_{aq}^- signal intensity.

What is noteworthy is that the spectra given by H-atoms formed upon S_1 excitation do not display any sign of a [PhO$^\bullet$···H$^\bullet$] geminate pair RPM signal contribution. Hence, the FT-EPR results provide no evidence of an in-cage H-atom formation step such as

$$[\mathrm{PhO}^\bullet\cdots\mathrm{e}_{\mathrm{aq}}^-] + \mathrm{H}^+ \rightarrow [\mathrm{PhO}^\bullet\cdots\mathrm{H}^\bullet] \rightarrow \mathrm{PhO}^\bullet + \mathrm{H}^\bullet$$

or

$$[\mathrm{PhOH}^+\cdots\mathrm{e}_{\mathrm{aq}}^-] \rightarrow [\mathrm{PhO}^\bullet\cdots\mathrm{H}^\bullet] \rightarrow \mathrm{PhO}^\bullet + \mathrm{H}^\bullet$$

It was noted in the Introduction that the quantum yield of H-atom formation as measured by H_2 evolution under steady-state irradiation conditions (pH 4−8, $\lambda_{ex} = 254$ nm) is ≤ 0.002.[2] Hydrated electrons produced by photoionization were scavenged by N_2O in these measurements so that H$^\bullet$ formation as a result of electron capture by protons in the bulk of the solution was eliminated. The FT-EPR measurements confirm that in the pH 7 to 3 range the presence of N_2O completely suppresses formation of H$^\bullet$.

IV.3. Formation of HPhOH$^\bullet$. Photoionization and H-atom formation initiated by excitation into the S_1 band is believed to occur via the relaxed singlet excited state.[2,3] Quantum yields of these reactions are significantly less than found for S_2 excitation. As a consequence, intersystem crossing (isc) to the triplet excited state can be an important S_1 decay channel.

Triplet-state formation accounts for formation of a cyclohexadienyl-type radical (cf. Figure 2) in a bimolecular hydrogen abstraction reaction involving ground-state phenol and triplet-state phenol. This reaction has been found as well for *p*-cresol and sesamol. In the case of sesamol, the triplet-state hydrogen abstraction reaction was found to be the only radical-producing reaction in neutral aqueous solution.[19]

That reaction 1 is the origin of the HPhOH$^\bullet$ radical is supported by the kinetics of signal growth (Figure 3b) and the effect of using D_2O as solvent (cf. Figure 2b) described in Section III.1. The A/E polarization pattern in the HPhOH$^\bullet$ spectrum is consistent with CIDEP generated by the [PhO$^\bullet$··· HPhOH$^\bullet$] radical pair "born" in the triplet state ($J < 0$).

V. Conclusions

FT-EPR measurements show that photoexcitation of aqueous solutions (pH 7−2) of phenol, *p*-cresol, and tyrosine in the S_2 absorption band ($\lambda_{ex} = 193$ nm) initiates two parallel reactions. One generating phenoxyl radicals and hydrated electrons,

$$^1\mathrm{PhOH}^*(S_2) \rightarrow [\mathrm{PhO}^\bullet\cdots\mathrm{e}_{\mathrm{aq}}^-] + \mathrm{H}^+ \rightarrow \mathrm{PhO}^\bullet + \mathrm{e}_{\mathrm{aq}}^- + \mathrm{H}^+ \quad (2)$$

the other phenoxyl radicals and hydrogen atoms by O−H bond cleavage,

$$^1\mathrm{PhOH}^*(S_2) \rightarrow [\mathrm{PhO}^\bullet\cdots\mathrm{H}^\bullet] \rightarrow \mathrm{PhO}^\bullet + \mathrm{H}^\bullet \quad (3)$$

The effect of electron scavenging by N_2O demonstrates that H-atoms are formed as well by the reaction of e_{aq}^- with H^+,

$$\mathrm{e}_{\mathrm{aq}}^- + \mathrm{H}^+ \rightarrow \mathrm{H}^\bullet \quad (4)$$

This reaction occurs following dissociation of the initially formed radical pair, [PhO$^\bullet$···e_{aq}^-], as evident from the fact that the spectrum of H$^\bullet$ shows spin polarization generated by the evolution of the spin state of this radical pair.

Reactions 2 and 3 are distinct in the spin polarization produced by the radical pairs [PhO$^\bullet$···e_{aq}^-] and [PhO$^\bullet$···H$^\bullet$]. Spin polarization from the ST_0 RPM involving [PhO$^\bullet$···H$^\bullet$] gives rise to an E/A pattern in the spectrum of H$^\bullet$. Due to the large hfcc of the H-atom, an additional net absorption contribution is generated by ST_{-1} mixing in the radical pair. The E/A* pattern is consistent with a reaction involving a singlet-state precursor generating a radical pair with $J < 0$.[5] The resonance peaks from PhO$^\bullet$ and e_{aq}^-, on the other hand, display an A/E pattern. If photoionization occurs via the singlet excited state, J in the radical pair must be positive. To account for this pattern in the case that $J < 0$, one has to invoke a triplet excited-state photoionization process.[5] Data from picosecond transient absorption measurements[12] combined with those given by a FT-EPR study[11] of photoionization at pH 11 indicate that photoionization occurs from the singlet excited state so that the reversal in polarization pattern must be due to a switch in the sign of J.

Excitation to S_1 ($\lambda_{ex} = 266$ nm) also produces PhO$^\bullet$, e_{aq}^-, and H$^\bullet$. In addition, FT-EPR spectra reveal a spectrum of a cyclohexadienyl radical that is formed in a triplet-state hydrogen abstraction reaction. The signal-to-noise of the FT-EPR spectra is considerably less than that obtained upon excitation in S_2, consistent with the reduced quantum yield of the photochemical reactions.[2,3]

The signal contributions from PhO$^\bullet$ and e_{aq}^- are similar to those observed with 193 nm excitation, but an increased net emission signal contribution in the spectrum from PhO$^\bullet$ may be due to the H-atom formation step. The H$^\bullet$ spectrum can be quenched by the addition of N_2O. This establishes that direct photoinduced bond cleavage does not contribute to H-atom formation, but that the observed H$^\bullet$ resonance peaks stem entirely from scavenging of e_{aq}^- by protons. The CIDEP pattern (A/E*) in the H-atom spectrum stems from the F-pair (ST_0, ST_{-1}) RPM. The spectra do not show any indication of a wavelength effect on the characteristics of the radical pairs [PhO$^\bullet$···e_{aq}^-] and [PhO$^\bullet$···H$^\bullet$].

Acknowledgment. Financial support for this work was provided by the Division of Chemical Sciences, Office of Basic Energy Sciences of the U.S. Department of Energy (DE-FG02-84ER-13242).

References and Notes

(1) For a recent review and leading references, see Richard C.; Grabner, G. In *The Handbook of Environmental Chemistry*, Vol. 2 Part L.; Boule P., Ed.; Springer-Verlag: Berlin, 1999; p 218.

(2) Grabner, G.; Köhler, G.; Zechner, J.; Getoff, N. *Photochem. Photobiol.* **1977**, *26*, 449.

(3) Köhler, G.; Getoff, N. *J. Chem. Soc., Faraday Trans. 1* **1976**, *73*, 2101.

(4) Goldschmidt, C. R.; Stein, G. *Chem. Phys. Lett.* **1970**, *6*, 299.

(5) For a review of CIDEP effects and leading references, see McLauchlan, K. A. In *Modern Pulsed and Continuous Wave Electron Spin Resonance*; Kevan, L., Bowman, M. K., Eds.; Wiley: New York, 1990; pp 285−364.

(6) Ohara, K.; Hirota, N.; Martino, D. M.; van Willigen, H. *J. Phys. Chem. A* **1998**, *102*, 5433.

(7) Kleverlaan, C. J.; Martino, D. M.; van Slageren, J.; van Willigen, H.; Stufkens, D. J.; Oskam, A. *Appl. Magn. Reson.* **1998**, *15*, 203.

(8) van Slageren, J.; Martino, D. M.; Kleverlaan, C. J.; Bussandri, A. P.; van Willigen, H.; Stufkens, D. J. *J. Phys. Chem. A* **2000**, *104*, 5969.

(9) Jeevarajan, A. S.; Fessenden, R. W. *J. Phys. Chem.* **1992**, *96*, 1520.

(10) Clancy, C. M. R.; Forbes, M. D. E. *Photochem. Photobiol.* **1999**, *69*, 16.

(11) Bussandri, A.; van Willigen, H. *J. Phys. Chem. A* **2001**, *105*, 4668.

(12) Mialocq, J.; Sutton, J.; Goujon, P. *J. Phys. Chem.* **1980**, *72*, 6338.

(13) Keene, J. P. *Radiat. Res.* **1964**, *22*, 1.

(14) Buxton, G.; Greenstock, C.; Helman, W.; Ross, A. B. *J. Phys. Chem. Ref. Data* **1988**, *17*, 513.

(15) Levstein, P. R.; van Willigen, H. *J. Chem. Phys.* **1991**, *95*, 900.

(16) de Beer, R.; van Ormondt, D. In *Advanced EPR: Applications in Biology and Biochemistry*; Hoff, A. J., Ed.; Elsevier: Amsterdam, 1989; pp 135−173.
(17) Neta, P.; Fessenden, R. W.; Schuler, R. *J. Phys. Chem.* **1971**, *75*, 1654.
(18) Fessenden, R. W.; Schuler, R. H. *J. Chem. Phys.* **1963**, *38*, 773.
(19) Bussandri, A.; van Willigen, H.; Nakagawa, K. *Appl. Magn. Reson.* **1999**, *17*, 577.
(20) (a) Smaller, B.; Avery, E. C.; Remko, J. R. *J. Chem. Phys.* **1971**, *55*, 2414. (b) Zechner, J.; Köhler, G.; Grabner, G.; Getoff, N. *Can. J. Chem.* **1980**, *58*, 2006.
(21) Adrian, F. *J. Chem. Phys.* **1971**, *54*, 3918.